

Measurement of the $e^+e^- \rightarrow \gamma\gamma(\gamma)$ cross section at LEP energies

DELPHI Collaboration

Abstract

The total and the differential cross sections for the reaction $e^+e^- \rightarrow \gamma\gamma(\gamma)$ have been measured with the DELPHI detector at LEP using an integrated luminosity of 36.9 pb^{-1} . The results agree with the QED predictions and consequently there is no evidence for non-standard channels with the same experimental signature. The lower limits obtained on the QED cutoff parameters are $\Lambda_+ > 143 \text{ GeV}$ and $\Lambda_- > 120 \text{ GeV}$, and the lower bound on the mass of an excited electron with an effective coupling constant $\lambda_\gamma = 1$ is $132 \text{ GeV}/c^2$. Upper limits on the branching ratios for the decays $Z^0 \rightarrow \gamma\gamma$, $Z^0 \rightarrow \pi^0\gamma$, $Z^0 \rightarrow \eta\gamma$ and $Z^0 \rightarrow \gamma\gamma\gamma$ have been determined to be 5.5×10^{-5} , 5.5×10^{-5} , 8.0×10^{-5} , and 1.7×10^{-5} respectively. All the limits are at the 95% confidence level.

(To be submitted to Physics Letters B)

P.Abreu²⁰, W.Adam⁷, T.Adye³⁷, E.Agasi³⁰, I.Ajinenko⁴², R.Aleksan³⁹, G.D.Alekseev¹⁴, P.Allport²¹,
 S.Almehed²³, F.M.L.Almeida Junior⁴⁷, S.J.Alvsvaag⁴, U.Amaldi⁷, A.Andreazza²⁷, P.Antilogus²⁴, W-D.Apel¹⁵,
 R.J.Apsimon³⁷, Y.Arnoud³⁹, B.Åsman⁴⁴, J-E.Augustin¹⁸, A.Augustinus³⁰, P.Baillon⁷, P.Bambade¹⁸,
 F.Barao²⁰, R.Barate¹², G.Barbiellini⁴⁶, D.Y.Bardin¹⁴, G.J.Barker³⁴, A.Baroncelli⁴⁰, O.Barring⁷, J.A.Barrio²⁵,
 W.Bartl⁵⁰, M.J.Bates³⁷, M.Battaglia¹³, M.Baubillier²², K-H.Becks⁵², M.Begalli³⁶, P.Beilliere⁶, P.Beltran⁹,
 A.C.Benvenuti⁵, M.Berggren¹⁸, D.Bertrand², F.Bianchi⁴⁵, M.Biggi⁴⁵, M.S.Bilenky¹⁴, P.Billoir²², J.Bjarne²³,
 D.Bloch⁸, J.Blocki⁵¹, S.Blyth³⁴, V.Bocci³⁸, P.N.Bogolubov¹⁴, T.Bolognese³⁹, M.Bonesini²⁷, W.Bonivento²⁷,
 P.S.L.Booth²¹, G.Borisov⁴², C.Bosio⁴⁰, B.Bostjancic⁴³, S.Bosworth³⁴, O.Botner⁴⁸, B.Bouquet¹⁸,
 C.Bourdarios¹⁸, T.J.V.Bowcock²¹, M.Bozzo¹¹, S.Braibant², P.Branchini⁴⁰, K.D.Brand³⁵, R.A.Brenner¹³,
 H.Briand²², C.Bricman², L.Brillault²², R.C.A.Brown⁷, J-M.Brunet⁶, L.Bugge³², T.Buran³², A.Buys⁷,
 J.A.M.A.Buytaert⁷, M.Caccia²⁷, M.Calvi²⁷, A.J.Camacho Rozas⁴¹, R.Campion²¹, T.Camporesi⁷, V.Canale³⁸,
 K.Cankocak⁴⁴, F.Cao², F.Carena⁷, P.Carrilho⁴⁷, L.Carroll²¹, R.Cases⁴⁹, C.Caso¹¹, M.V.Castillo Gimenez⁴⁹,
 A.Cattai⁷, F.R.Cavallo⁵, L.Cerrito³⁸, V.Chabaud⁷, A.Chan¹, M.Chapkin⁴², Ph.Charpentier⁷, J.Chauveau²²,
 P.Checchia³⁵, G.A.Chelkov¹⁴, L.Chevalier³⁹, P.Chliapnikov⁴², V.Chorowicz²², J.T.M.Chrin⁴⁹, V.Cindro⁴³,
 P.Collins³⁴, J.L.Contreras¹⁸, R.Contri¹¹, E.Cortina⁴⁹, G.Cosme¹⁸, F.Couchot¹⁸, H.B.Crawley¹, D.Crennell³⁷,
 G.Crosetti¹¹, J.Cuevas Maestro³³, S.Czellar¹³, E.Dahl-Jensen²⁸, J.Dahm⁵², B.Dalmagne¹⁸, M.Dam³²,
 G.Damgaard²⁸, E.Daubie², A.Daum¹⁵, P.D.Dauncey⁷, M.Davenport⁷, J.Davies²¹, W.Da Silva²², C.Defoix⁶,
 P.Delpierre²⁶, N.Demaria³⁴, A.De Angelis⁷, H.De Boeck², W.De Boer¹⁵, S.De Brabandere², C.De Clercq²,
 M.D.M.De Fez Laso⁴⁹, C.De La Vaissiere²², B.De Lotto⁴⁶, A.De Min²⁷, L.De Paula⁴⁷, H.Dijkstra⁷,
 L.Di Ciaccio³⁸, F.Djama⁸, J.Dolbeau⁶, M.Donszelmann⁷, K.Doroba⁵¹, M.Dracos⁸, J.Drees⁵², M.Dris³¹,
 Y.Dufour⁷, F.Dupont¹², D.Edsall¹, L-O.Eek⁴⁸, R.Ehret¹⁵, T.Ekelof⁴⁸, G.Ekspong⁴⁴, A.Elliot Peisert⁷,
 M.Elsing⁵², J-P.Engel⁸, N.Ershaidat²², M.Espirito Santo²⁰, V.Falaleev⁴², D.Fassouliotis³¹, M.Feindt⁷,
 A.Ferrer⁴⁹, T.A.Filippas³¹, A.Firestone¹, H.Foeth⁷, E.Fokitis³¹, F.Fontanelli¹¹, K.A.J.Forbes²¹, F.Formenti⁷,
 J-L.Fousset²⁶, S.Francon²⁴, B.Franek³⁷, P.Frenkiel⁶, D.C.Fries¹⁵, A.G.Frodesen⁴, R.Fruhworth⁵⁰,
 F.Fulda-Quenzer¹⁸, H.Furstenau⁷, J.Fuster⁷, D.Gamba⁴⁵, M.Gandelman¹⁷, C.Garcia⁴⁹, J.Garcia⁴¹, C.Gaspar⁷,
 U.Gasparini³⁵, Ph.Gavillet⁷, E.N.Gazis³¹, J-P.Gerber⁸, P.Giacomelli⁷, D.Gillespie⁷, R.Gokiel⁵¹, B.Golob⁴³,
 V.M.Golovatyuk¹⁴, J.J.Gomez Y Cadenas⁷, G.Gopal³⁷, L.Gorn¹, M.Gorski⁵¹, V.Gracco¹¹, F.Grad²,
 E.Graziani⁴⁰, G.Grosdidier¹⁸, B.Grossetete²², P.Gunnarsson⁴⁴, J.Guy³⁷, U.Haeding¹⁵, F.Hahn⁵², M.Hahn⁴⁴,
 S.Hahn⁵², S.Haider³⁰, Z.Hajduk¹⁶, A.Hakansson²³, A.Hallgren⁴⁸, K.Hamacher⁵², G.Hamel De Monchenault³⁹,
 W.Hao³⁰, F.J.Harris³⁴, V.Hedberg²³, R.Henriques²⁰, J.J.Hernandez⁴⁹, J.A.Hernando⁴⁹, P.Herquet², H.Herr⁷,
 T.L.Hessing²¹, C.O.Higgins²¹, E.Higon⁴⁹, H.J.Hilke⁷, T.S.Hill¹, S.D.Hodgson³⁴, S-O.Holmgren⁴⁴, P.J.Holt³⁴,
 D.Holthuizen³⁰, P.F.Honore⁶, M.Houlden²¹, J.Hrubic⁵⁰, K.Huet², K.Hultqvist⁴⁴, P.Ioannou³, P-S.Iversen⁴,
 J.N.Jackson²¹, R.Jacobsson⁴⁴, P.Jalocha¹⁶, G.Jarlskog²³, P.Jarry³⁹, B.Jean-Marie¹⁸, E.K.Johansson⁴⁴,
 M.Jonker⁷, L.Jonsson²³, P.Juillot⁸, M.Kaiser¹⁵, G.Kalmus³⁷, F.Kapusta²², M.Karlsson⁴⁴, E.Karvelas⁹,
 A.Katargin⁴², S.Katsanevas³, E.C.Katsoufis³¹, R.Keranen⁷, B.A.Khomenko¹⁴, N.N.Khovanski¹⁴, B.King²¹,
 N.J.Kjaer²⁸, H.Klein⁷, A.Klovning⁴, P.Kluit³⁰, A.Koch-Mehrin⁵², J.H.Koehne¹⁵, B.Koene³⁰, P.Kokkinias⁹,
 M.Koratzinos³², K.Korcy¹⁶, A.V.Korytov¹⁴, V.Kostioukhine⁴², C.Kourkoumelis³, O.Kouznetsov¹⁴,
 P.H.Kramer⁵², M.Krammer⁵⁰, C.Kreuter¹⁵, J.Krolikowski⁵¹, I.Kronkvist²³, W.Krupinski¹⁶, K.Kulka⁴⁸,
 K.Kurvinen¹³, C.Lacasta⁴⁹, C.Lambropoulos⁹, J.W.Lamsa¹, L.Lanceri⁴⁶, P.Langefeld⁵², V.Lapin⁴², I.Last²¹,
 J-P.Laugier³⁹, R.Lauhakangas¹³, G.Leder⁵⁰, F.Ledroit¹², R.Leitner²⁹, Y.Lemoigne³⁹, J.Lemonne², G.Lenzen⁵²,
 V.Lepeltier¹⁸, T.Lesiak¹⁶, J.M.Levy⁸, E.Lieb⁵², D.Liko⁵⁰, R.Lindner⁵², A.Lipniacka¹⁸, I.Lippi³⁵, B.Loerstad²³,
 M.Lokajicek¹⁰, J.G.Loken³⁴, A.Lopez-Fernandez⁷, M.A.Lopez Aguera⁴¹, M.Los³⁰, D.Loukas⁹, J.J.Lozano⁴⁹,
 P.Lutz⁶, L.Lyons³⁴, G.Maehlum¹⁵, J.Maillard⁶, A.Maio²⁰, A.Maltesos⁹, F.Mandl⁵⁰, J.Marco⁴¹, B.Marechal⁴⁷,
 M.Margoni³⁵, J-C.Marin⁷, C.Mariotti⁴⁰, A.Markou⁹, T.Maron⁵², S.Marti⁴⁹, C.Martinez-Rivero⁴¹,
 F.Martinez-Vidal⁴⁹, F.Matorras⁴¹, C.Matteuzzi²⁷, G.Matthiae³⁸, M.Mazzucato³⁵, M.Mc Cubbin²¹, R.Mc Kay¹,
 R.Mc Nulty²¹, J.Medbo⁴⁸, C.Meroni²⁷, W.T.Meyer¹, M.Michelotto³⁵, E.Migliore⁴⁵, I.Mikulec⁵⁰, L.Mirabito²⁴,
 G.V.Mitselmakher¹⁴, U.Mjoernmark²³, T.Moa⁴⁴, R.Moeller²⁸, K.Moenig⁷, M.R.Monge¹¹, P.Morettini¹¹,
 H.Mueller¹⁵, W.J.Murray³⁷, B.Muryn¹⁶, G.Myatt³⁴, F.Naraghi¹², F.L.Navarria⁵, P.Negri²⁷, S.Nemecsek¹⁰,
 W.Neumann⁵², N.Neumeister⁵⁰, R.Nicolaidou³, B.S.Nielsen²⁸, P.E.S.Nilsen⁴, P.Niss⁴⁴, A.Nomerotski³⁵,
 V.Obraztsov⁴², A.G.Olshevski¹⁴, R.Orava¹³, A.Ostankov⁴², K.Osterberg¹³, A.Ouraou³⁹, P.Paganini¹⁸,
 M.Paganoni²⁷, R.Pain²², H.Palka¹⁶, Th.D.Papadopoulou³¹, L.Pape⁷, F.Parodi¹¹, A.Passeri⁴⁰, M.Pegoraro³⁵,
 J.Pennanen¹³, L.Peralta²⁰, H.Pernegger⁵⁰, M.Pernicka⁵⁰, A.Perrotta⁵, C.Petridou⁴⁶, A.Petrolini¹¹, G.Piana¹¹,
 F.Pierre³⁹, M.Pimenta²⁰, S.Plaszczynski¹⁸, O.Podobrin¹⁵, M.E.Pol¹⁷, G.Polok¹⁶, P.Poropat⁴⁶, V.Pozdniakov¹⁴,
 M.Prest⁴⁶, P.Privitera³⁸, A.Pullia²⁷, D.Radojicic³⁴, S.Ragazzi²⁷, H.Rahmani³¹, J.Rames¹⁰, P.N.Ratoff¹⁹,
 A.L.Read³², M.Reale⁵², P.Rebecchi¹⁸, N.G.Redaeli²⁷, M.Regler⁵⁰, D.Reid⁷, P.B.Renton³⁴, L.K.Resvanis³,
 F.Richard¹⁸, J.Richardson²¹, J.Ridky¹⁰, G.Rinaudo⁴⁵, A.Romero⁴⁵, I.Roncagliolo¹¹, P.Ronchese³⁵,
 E.I.Rosenberg¹, E.Rosso⁷, P.Roudeau¹⁸, T.Rovelli⁵, W.Ruckstuhl³⁰, V.Ruhlmann-Kleider³⁹, A.Ruiz⁴¹,
 K.Rybicki¹⁶, H.Saarikko¹³, Y.Sacquin³⁹, G.Sajot¹², J.Salt⁴⁹, J.Sanchez²⁵, M.Sannino¹¹, S.Schael⁷,

H.Schneider¹⁵, M.A.E.Schyns⁵², G.Sciolla⁴⁵, F.Scuri⁴⁶, A.M.Segar³⁴, A.Seitz¹⁵, R.Sekulin³⁷, M.Sessa⁴⁶, R.Seufert¹⁵, R.C.Shellard³⁶, I.Siccama³⁰, P.Siegrist³⁹, S.Simonetti¹¹, F.Simonetto³⁵, A.N.Sisakian¹⁴, G.Skjevling³², G.Smadja²⁴, N.Smirnov⁴², O.Smirnova¹⁴, G.R.Smith³⁷, R.Sosnowski⁵¹, D.Souza-Santos³⁶, T.Spaso²⁰, E.Spiriti⁴⁰, S.Squarcia¹¹, H.Staek⁵², C.Stanescu⁴⁰, S.Stapnes³², G.Stavropoulos⁹, K.Stepaniak⁵¹, F.Stichelbaut⁷, A.Stocchi¹⁸, J.Strauss⁵⁰, J.Straver⁷, R.Strub⁸, B.Stugu⁴, M.Szczekowski⁵¹, M.Szeptycka⁵¹, P.Szymanski⁵¹, T.Tabarelli²⁷, O.Tchikilev⁴², G.E.Theodosiou⁹, Z.Thome⁴⁷, A.Tilquin²⁶, J.Timmermans³⁰, V.G.Timofeev¹⁴, L.G.Tkatchev¹⁴, T.Todorov⁸, D.Z.Toet³⁰, A.Tomaradze², B.Tome²⁰, E.Torassa⁴⁵, L.Tortora⁴⁰, D.Treille⁷, W.Trischuk⁷, G.Tristram⁶, C.Troncon²⁷, A.Tsirou⁷, E.N.Tsyganov¹⁴, M.Turala¹⁶, M-L.Turluer³⁹, T.Tuuva¹³, I.A.Tyapkin²², M.Tyndel³⁷, S.Tzamarias²¹, B.Ueberschaer⁵², S.Ueberschaer⁵², O.Ullaland⁷, V.Uvarov⁴², G.Valenti⁵, E.Vallazza⁷, J.A.Valls Ferrer⁴⁹, C.Vander Velde², G.W.Van Apeldoorn³⁰, P.Van Dam³⁰, M.Van Der Heijden³⁰, W.K.Van Doninck², J.Van Eldik³⁰, P.Vaz⁷, G.Vegni²⁷, L.Ventura³⁵, W.Venus³⁷, F.Verbeure², M.Verlato³⁵, L.S.Vertogradov¹⁴, D.Vilanova³⁹, P.Vincent²⁴, L.Vitale⁴⁶, E.Vlasov⁴², A.S.Vodopyanov¹⁴, M.Vollmer⁵², M.Voutilainen¹³, V.Vrba¹⁰, H.Wahlen⁵², C.Walck⁴⁴, F.Waldner⁴⁶, A.Wehr⁵², M.Weierstall⁵², P.Weilhammer⁷, A.M.Wetherell⁷, J.H.Wickens², M.Wielers¹⁵, G.R.Wilkinson³⁴, W.S.C.Williams³⁴, M.Winter⁸, M.Witek⁷, G.Wormser¹⁸, K.Woschnagg⁴⁸, A.Zaitsev⁴², A.Zalewska¹⁶, P.Zalewski⁵¹, D.Zavrtanik⁴³, E.Zevgolatakos⁹, N.I.Zimin¹⁴, M.Zito³⁹, D.Zontar⁴³, R.Zuberi³⁴, G.Zumerle³⁵

¹ Ames Laboratory and Department of Physics, Iowa State University, Ames IA 50011, USA

² Physics Department, Univ. Instelling Antwerpen, Universiteitsplein 1, B-2610 Wilrijk, Belgium and IHHE, ULB-VUB, Pleinlaan 2, B-1050 Brussels, Belgium

³ and Faculté des Sciences, Univ. de l'Etat Mons, Av. Maistriau 19, B-7000 Mons, Belgium

⁴ Physics Laboratory, University of Athens, Solonos Str. 104, GR-10680 Athens, Greece

⁵ Dipartimento di Fisica, Università di Bologna and INFN, Via Irnerio 46, I-40126 Bologna, Italy

⁶ Collège de France, Lab. de Physique Corpusculaire, IN2P3-CNRS, F-75231 Paris Cedex 05, France

⁷ CERN, CH-1211 Geneva 23, Switzerland

⁸ Centre de Recherche Nucléaire, IN2P3 - CNRS/ULP - BP20, F-67037 Strasbourg Cedex, France

⁹ Institute of Nuclear Physics, N.C.S.R. Demokritos, P.O. Box 60228, GR-15310 Athens, Greece

¹⁰ FZU, Inst. of Physics of the C.A.S. High Energy Physics Division, Na Slovance 2, CS-180 40, Praha 8, Czechoslovakia

¹¹ Dipartimento di Fisica, Università di Genova and INFN, Via Dodecaneso 33, I-16146 Genova, Italy

¹² Institut des Sciences Nucléaires, IN2P3-CNRS, Université de Grenoble 1, F-38026 Grenoble, France

¹³ Research Institute for High Energy Physics, SEFT, P.O. Box 9, FIN-00014 University of Helsinki, Finland

¹⁴ Joint Institute for Nuclear Research, Dubna, Head Post Office, P.O. Box 79, 101 000 Moscow, Russian Federation

¹⁵ Institut für Experimentelle Kernphysik, Universität Karlsruhe, Postfach 6980, D-76128 Karlsruhe, Germany

¹⁶ High Energy Physics Laboratory, Institute of Nuclear Physics, Ul. Kawioro 26a, PL-30055 Krakow 30, Poland

¹⁷ Centro Brasileiro de Pesquisas Físicas, rua Xavier Sigaud 150, RJ-22290 Rio de Janeiro, Brazil

¹⁸ Université de Paris-Sud, Lab. de l'Accélérateur Linéaire, IN2P3-CNRS, Bat 200, F-91405 Orsay, France

¹⁹ School of Physics and Materials, University of Lancaster, Lancaster LA1 4YB, UK

²⁰ LIP, IST, FCUL - Av. Elias Garcia, 14-1º, P-1000 Lisboa Codex, Portugal

²¹ Department of Physics, University of Liverpool, P.O. Box 147, Liverpool L69 3BX, UK

²² LPNHE, IN2P3-CNRS, Universités Paris VI et VII, Tour 33 (RdC), 4 place Jussieu, F-75252 Paris Cedex 05, France

²³ Department of Physics, University of Lund, Sölvegatan 14, S-22363 Lund, Sweden

²⁴ Université Claude Bernard de Lyon, IPNL, IN2P3-CNRS, F-69622 Villeurbanne Cedex, France

²⁵ Universidad Complutense, Avda. Complutense s/n, E-28040 Madrid, Spain

²⁶ Univ. d'Aix - Marseille II - CPP, IN2P3-CNRS, F-13288 Marseille Cedex 09, France

²⁷ Dipartimento di Fisica, Università di Milano and INFN, Via Celoria 16, I-20133 Milan, Italy

²⁸ Niels Bohr Institute, Blegdamsvej 17, DK-2100 Copenhagen 0, Denmark

²⁹ NC, Nuclear Centre of MFF, Charles University, Areal MFF, V Holesovickach 2, CS-180 00, Praha 8, Czechoslovakia

³⁰ NIKHEF-H, Postbus 41882, NL-1009 DB Amsterdam, The Netherlands

³¹ National Technical University, Physics Department, Zografou Campus, GR-15773 Athens, Greece

³² Physics Department, University of Oslo, Blindern, N-1000 Oslo 3, Norway

³³ Dpto. Fisica, Univ. Oviedo, C/P.Jimenez Casas, S/N-33006 Oviedo, Spain

³⁴ Department of Physics, University of Oxford, Keble Road, Oxford OX1 3RH, UK

³⁵ Dipartimento di Fisica, Università di Padova and INFN, Via Marzolo 8, I-35131 Padua, Italy

³⁶ Depto. de Fisica, Pontificia Univ. Católica, C.P. 38071 RJ-22453 Rio de Janeiro, Brazil

³⁷ Rutherford Appleton Laboratory, Chilton, Didcot OX11 0QX, UK

³⁸ Dipartimento di Fisica, Università di Roma II and INFN, Tor Vergata, I-00173 Rome, Italy

³⁹ Centre d'Etude de Saclay, DSM/DAPNIA, F-91191 Gif-sur-Yvette Cedex, France

⁴⁰ Istituto Superiore di Sanità, Ist. Naz. di Fisica Nucl. (INFN), Viale Regina Elena 299, I-00161 Rome, Italy

⁴¹ C.E.A.F.M., C.S.I.C. - Univ. Cantabria, Avda. los Castros, S/N-39006 Santander, Spain

⁴² Inst. for High Energy Physics, Serpukov P.O. Box 35, Protvino, (Moscow Region), Russian Federation

⁴³ J. Stefan Institute and Department of Physics, University of Ljubljana, Jamova 39, SI-61000 Ljubljana, Slovenia

⁴⁴ Fysikum, Stockholm University, Box 6730, S-113 85 Stockholm, Sweden

⁴⁵ Dipartimento di Fisica Sperimentale, Università di Torino and INFN, Via P. Giuria 1, I-10125 Turin, Italy

⁴⁶ Dipartimento di Fisica, Università di Trieste and INFN, Via A. Valerio 2, I-34127 Trieste, Italy

and Istituto di Fisica, Università di Udine, I-33100 Udine, Italy

⁴⁷ Univ. Federal do Rio de Janeiro, C.P. 68528 Cidade Univ., Ilha do Fundão BR-21945-970 Rio de Janeiro, Brazil

⁴⁸ Department of Radiation Sciences, University of Uppsala, P.O. Box 535, S-751 21 Uppsala, Sweden

⁴⁹ IFIC, Valencia-CSIC, and D.F.A.M.N., U. de Valencia, Avda. Dr. Moliner 50, E-46100 Burjassot (Valencia), Spain

⁵⁰ Institut für Hochenergiephysik, Österr. Akad. d. Wissensch., Nikolsdorfergasse 18, A-1050 Vienna, Austria

⁵¹ Inst. Nuclear Studies and University of Warsaw, Ul. Hoza 69, PL-00681 Warsaw, Poland

⁵² Fachbereich Physik, University of Wuppertal, Postfach 100 127, D-5600 Wuppertal 1, Germany

1 Introduction

The reaction $e^+e^- \rightarrow \gamma\gamma(\gamma)$ provides a clean test of QED at LEP energies and it is well suited to detect the presence of non-standard physics. A previous letter from the DELPHI collaboration [1] reported a study of this reaction based on 4.7 pb^{-1} ; similar results were published by other LEP collaborations [2]. In this letter an improved measurement of the $e^+e^- \rightarrow \gamma\gamma(\gamma)$ cross section is reported using the data collected by DELPHI during the 1991 and 1992 runs. The results published in Ref.[1] were also included in the fits to the differential and total cross sections, giving a total integrated luminosity of 36.9 pb^{-1} for the whole 1990-1992 period.

2 Apparatus

A detailed description of the DELPHI detector can be found in Ref.[3]. The present analysis was mainly based on the measurement of the electromagnetic energy clusters [4] in the barrel electromagnetic calorimeter, the High density Projection Chamber (HPC), and in the Forward ElectroMagnetic Calorimeter (FEMC) as well as on the capability of vetoing the charged particles using the tracking devices. In addition to the track reconstruction in the Time Projection Chamber (TPC), Inner Detector (ID) and Outer Detector (OD), a very efficient way of rejecting final states which include charged particles is to use hits reconstructed in the Vertex Detector (VD).

The Vertex Detector consists of three layers of silicon strips at radial distances of 6.5 cm, 9 cm and 11 cm from the nominal beam crossing position. They provide measurements of the $R\phi$ coordinate (R is the radial coordinate and ϕ is the azimuthal angle about the beam axis) with an absolute hit resolution of 8 microns in the plane transverse to the beam axis, and cover the region of polar angle (hereafter called θ) between 40° and 140° . The ID and the TPC cover polar angles $20^\circ < \theta < 160^\circ$, the OD covers the range $43^\circ < \theta < 137^\circ$. The HPC covers the region between 40° and 140° , and the FEMC the ranges $10^\circ < \theta < 36^\circ$ and $144^\circ < \theta < 170^\circ$. The hadron calorimeter (HCAL), which covers the entire barrel and endcap regions over the range $10^\circ < \theta < 170^\circ$, was used to reject cosmic rays. The Small Angle Tagger (SAT) and the Very Small Angle Tagger (VSAT) were used to measure the luminosity.

The barrel electromagnetic energy trigger was based on data from the HPC, from the barrel Time Of Flight counters (TOF) and from the Outer Detector (for photons converted before the HPC). The efficiency was estimated, using an independent track trigger, as the ratio of e^+e^- final state events with track as well as electromagnetic energy trigger to the number of e^+e^- events with a track trigger and it was $(99.9 \pm .05)\%$.

3 Event selection and analysis

Only the periods when the HPC, TPC and SAT were fully operational and when the VD was taking data were considered. They correspond to integrated luminosities in the 1991 and 1992 runs of 9.3 pb^{-1} and of 22.8 pb^{-1} respectively. The data of 1991 were collected at various LEP centre-of-mass energies, whereas the whole 1992 run was made at a single energy near the peak of the Z^0 resonance.

The most significant improvement to the analysis, with respect to the previous one [1], was the rejection of charged particle final states (mainly e^+e^- events which are produced at a rate which is more than fifty times higher than the signal) based on a Vertex Detector

track search; therefore the analysis was restricted to the barrel region. The forward region was used only in the search for $Z^0 \rightarrow \gamma\gamma\gamma$ events described in section 6. In simple topologies with high momentum particles, such as the leptonic decays of Z^0 , the Vertex Detector is very effective in finding track elements, consisting of two or more hits, almost independently of the other tracking devices. In order to reject e^+e^- events, it was required that there must be one hit in at least two of the three VD layers in one hemisphere, and that the hits must be aligned with the beam spot. In events where the charged particles were highly collimated in a back-to-back topology, the VD requirement of two hits in both hemispheres was relaxed to allow one hit in one of the hemispheres. The efficiency for reconstructing both VD tracks in a e^+e^- event using these algorithms was evaluated from the data by counting the number of such events having two tracks reconstructed in the TPC and one or both VD tracks missing. The efficiency for reconstructing two VD tracks was measured to be $99.67 \pm 0.04\%$.

Events were selected as $\gamma\gamma(\gamma)$ candidates if they satisfied the following criteria :

- at least one electromagnetic energy cluster with $30 < E < 65$ GeV and at least one other with $25 < E < 65$ GeV, both in the HPC;
- both energy clusters in the region $42^\circ < \theta < 88^\circ$ or $92^\circ < \theta < 138^\circ$;
- the azimuth ϕ of the impact point of the most energetic photon of a randomly chosen hemisphere more than 1° away from the boundaries of HPC modules;
- the acollinearity between the two most energetic clusters smaller than 30° ;
- no tracks reconstructed in the Vertex Detector corresponding to the HPC clusters ($\pm 2^\circ$ in ϕ);
- at least one hemisphere where there were no tracks reconstructed in the other tracking devices (hereafter these tracks will be called TK) that extrapolated to within 5 cm to the mean beam crossing point and had momentum higher than 1 GeV/c.

The energy cuts given above are those that were used for the events taken at the peak of the Z^0 resonance; outside the peak they were scaled according to the LEP centre-of-mass energy. The cut on VD tracks excluded $\gamma\gamma(\gamma)$ events with a photon which converted into e^+e^- before or in the region of sensitivity of the Vertex Detector. The cut on TK's was made to remove e^+e^- events with both VD tracks missing. Events with anomalously high numbers of tracks (> 10) not pointing to the vertex or with activity in two hemispheres of the Hadron Calorimeter were visually examined (3 events in the whole data set). They were identified as cosmic ray events and removed from the data sample.

After applying these requirements, samples of 125 and 323 events were obtained from the 1991 and 1992 data sets, respectively. The ability of these selection criteria to separate $\gamma\gamma(\gamma)$ events from the e^+e^- background can be seen in Fig.1 showing the difference in azimuth ($180^\circ - \Delta\phi$) between the two most energetic HPC clusters for both types of events. The $\gamma\gamma(\gamma)$ events do not exhibit the effect of the magnetic field bending as e^+e^- events do.

The advantage of using the Vertex Detector hits to reject e^+e^- events depends on the low probability ($< 1\%$) for a photon to convert before or within the Vertex Detector sensitive region, which could be evaluated from the Monte Carlo program with sufficient precision. The single photon conversion probability after the VD sensitive region was evaluated to be well below 10% both in the real and simulated data. Therefore the probability of losing $\gamma\gamma(\gamma)$ events from double photon conversion giving at least one TK per hemisphere was also small. The efficiency loss due to the energy requirements and the dead zones between HPC modules was determined in different θ intervals with a sample of 24046 generated $\gamma\gamma(\gamma)$ events [5] processed through the DELPHI detector simulation [6] and the same analysis chain as the real data. The efficiency obtained from the simulated

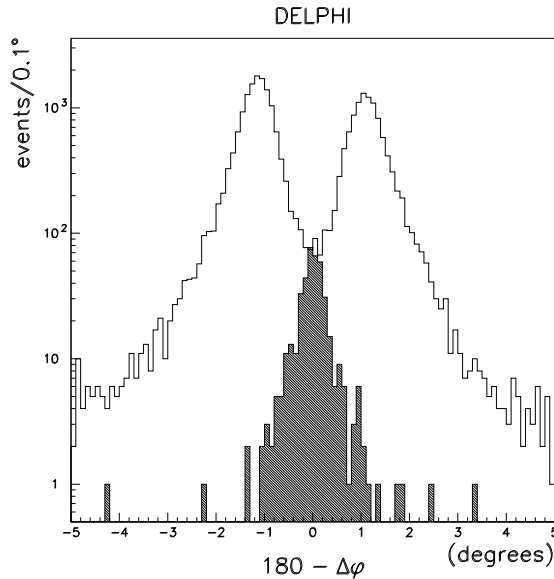


Figure 1: Distribution of the difference $180^\circ - \Delta\phi$ between the two most energetic HPC clusters for e^+e^- (white area) and $\gamma\gamma(\gamma)$ events (hatched area). The difference in height between the two e^+e^- peaks reflects the physical forward-backward asymmetry of such events.

data was corrected by a factor 1.035 ± 0.018 to take into account an inaccuracy on the simulation of the shower position reconstruction near the HPC dead regions. The global efficiency for accepting $\gamma\gamma(\gamma)$ events, integrated over the whole acceptance region, was then $(84.9 \pm 1.7)\%$, where the error includes the statistics of the simulated data and the uncertainty on the previous correction.

The only possible significant background was the small fraction of e^+e^- events (or τ events with high electromagnetic energy) missing both sets of VD hits and at least one TK. In order to quantify this background, e^+e^- events with two back-to-back track elements in the Vertex Detector were selected. The number of events with no TK in one hemisphere was then compared with the total number of events. Given the high efficiency of the VD, the corresponding background in the $\gamma\gamma(\gamma)$ sample was negligible (< 1 event) and was taken into account only as a contribution of $\pm 0.2\%$ to the systematic error. A similar result was obtained using events generated with the BABAMC Monte Carlo program[7].

The total systematic error, obtained by summing the uncertainties in the efficiency corrections and in the background subtraction and the $\pm 0.7\%$ uncertainty in the luminosity measurement[8] ($\pm 0.6\%$ in the 1991 data), was $\pm 2.1\%$.

Table 1 summarizes the integrated luminosity, the number of selected events and the corresponding cross sections (in the angular range $42^\circ < \theta < 90^\circ$) versus the centre-of-mass energy. The 1990 results are scaled with respect to those of Ref.[1] according to a $+1.6\%$ change in the luminosity after a re-analysis of the 1990 luminosity data [8]. The cross section at the mean of the centre-of-mass energies, weighted by the luminosity at each point, is also given. Some of the off-peak points are lower than the expected values. A check was done in order to find possible variations on the detection efficiency or specific losses at those points. No such effects were found and therefore the deviations are attributed to statistical fluctuations of small numbers of events. Table 2 summa-

\sqrt{s} (GeV)			σ_0 (pb)	σ (pb)	Int.Lumi (pb ⁻¹)	Number of events
1990	1991	1992				
88.223			19.6	$12.4^{+12.0}_{-3.8}$.332	3
	88.465		19.5	$14.3^{+7.1}_{-3.5}$.709	8
89.222			19.2	$11.4^{+11.1}_{-3.5}$.361	3
	89.460		19.1	$6.7^{+6.5}_{-2.0}$.566	3
	90.208		18.8	$16.2^{+8.7}_{-4.1}$.546	7
90.217			18.8	$18.1^{+12.2}_{-5.0}$.378	5
91.217			18.3	15.4 ± 2.9	2.490	28
	91.225		18.3	20.0 ± 2.1	5.567	88
		91.278	18.3	17.9 ± 1.0	22.83	323
	91.954		18.1	$19.2^{+8.2}_{-4.4}$.660	10
92.209			17.9	$17.1^{+11.7}_{-4.7}$.400	5
	92.953		17.7	$10.4^{+7.1}_{-2.9}$.606	5
93.208			17.6	$25.9^{+15.5}_{-6.8}$.318	6
	93.703		17.4	$7.8^{+6.2}_{-2.3}$.647	4
94.202			17.2	$14.8^{+10.0}_{-4.1}$.464	5
91.25			18.3	17.4 ± 0.8	36.87	503

Table 1: The lowest order $e^+e^- \rightarrow \gamma\gamma$ QED predictions (σ_0), the measured cross sections (σ), the integrated luminosities and the number of detected events at different centre-of-mass energies. The quoted errors are statistical only computed following the Bayesian approach (central interval) for small number of events [9]. They do not include the overall normalization errors of 2.1 % (3% in 1990). The 1990 results are scaled with respect to those of Ref.[1] according to a luminosity re-analysis. The cross section at the mean of the centre-of-mass energies, weighted by the luminosity at each point, is also given. The cross sections correspond to the angular range $42^\circ < \theta < 90^\circ$; the measured cross sections have been corrected for radiative effects.

izes the number of events and the corresponding differential cross section, corrected for the angular dependent detection efficiency, as a function of $\cos \theta$, summed over all the energies. The cosine of the scattering angle is defined as $\cos \theta = \left| \frac{\cos \frac{1}{2}(\theta_1 + \pi - \theta_2)}{\cos \frac{1}{2}(\theta_1 - \pi + \theta_2)} \right|$ where θ_1 and θ_2 are, respectively, the polar angles of the two most energetic photons. This definition has the advantage of not being sensitive to the collinear initial state radiation. The measured cross sections reported in both tables were obtained after subtracting the radiative corrections to order α^3 [5]. The lowest order QED predictions are included for comparison.

4 Test of QED

The total and differential cross sections with radiative corrections subtracted are shown in Figs. 2 and 3 respectively, together with the lowest order QED predictions. Only statistical errors are shown. The average cross section at the mean centre-of-mass energy is also shown in Fig.2.

$\cos \theta$	$d\sigma_0/d\Omega$ (pb/sr)	$d\sigma/d\Omega$ (pb/sr)	Number of events
0.035-0.136	2.53	2.69 ± 0.43	40
0.136-0.237	2.68	2.10 ± 0.35	35
0.237-0.338	2.95	2.71 ± 0.40	46
0.338-0.440	3.39	3.25 ± 0.43	57
0.440-0.541	4.08	3.44 ± 0.44	62
0.541-0.642	5.20	5.36 ± 0.55	94
0.642-0.743	7.15	7.28 ± 0.69	112
0.00-0.20	2.56	$3.2^{+1.2}_{-0.7}$	12
0.20-0.40	3.01	$3.6^{+1.1}_{-0.7}$	17
0.40-0.60	4.22	$2.7^{+1.0}_{-0.6}$	12
0.60-0.74	6.71	$4.4^{+1.5}_{-0.9}$	14
0.82-0.87	15.32	$9.6^{+5.1}_{-2.4}$	7

Table 2: The lowest order $e^+e^- \rightarrow \gamma\gamma$ QED predictions ($d\sigma_0/d\Omega$), the measured differential cross sections ($d\sigma/d\Omega$) and the number of detected events at different angles. The last five lines correspond to the 1990 published results scaled according to the luminosity re-analysis. The quoted errors are statistical only. The measured cross sections have been corrected for radiative effects.

Possible deviations from QED are usually parametrized by adding to the QED differential cross section a term depending on the cutoff parameters Λ_+ or Λ_- [10,11] :

$$\frac{d\sigma}{d\Omega} = \frac{\alpha^2}{s} \frac{1 + \cos^2 \theta}{1 - \cos^2 \theta} \left(1 \pm \frac{s^2}{2\Lambda_{\pm}^4} (1 - \cos^2 \theta) \right) \quad (1)$$

A maximum likelihood fit to the measured differential cross sections gave, for the parameter $\eta = 1/\Lambda^4$, a central value $\eta = (-0.20 \pm 0.16) \times 10^{-8} \text{ GeV}^{-4}$. This corresponds to lower limits at the 95% confidence level of $\Lambda_+ > 143 \text{ GeV}$ and $\Lambda_- > 120 \text{ GeV}$; these are shown as the dashed and dotted lines in Fig. 3. The overall normalization error of 2.1% was taken into account in the fitting procedure. The re-analysed 1990 results [1] were also included in the fit with a normalization error of $\pm 3\%$.

For these and the following limits, the confidence level was obtained by normalizing the probability to the integral over the region of definition of the parameters, as explained in Ref.[12]. The measured values and their errors are quoted, even though they are unphysical, in order to allow them to be combined with the results of other experiments and to permit the evaluation of the confidence level by alternative methods[13].

5 Search for rare Z^0 decays into neutral states.

A possible deviation of the measured cross section from the QED prediction at Z^0 energies could be interpreted as evidence for rare Z^0 decays, such as $Z^0 \rightarrow \gamma\gamma$ (theoretically forbidden[14]), $Z^0 \rightarrow \pi^0\gamma$ or $Z^0 \rightarrow \eta\gamma$ (with a branching ratio in the range 10^{-11} to 10^{-10} in the Standard Model [15]), all of which have a similar experimental signature since the neutral decay of a high energy meson was not distinguished from the passage of a single photon. This possibility was tested by analyzing the dependence of the total cross section on the centre-of-mass energy. The cross section was fitted to the sum of the QED

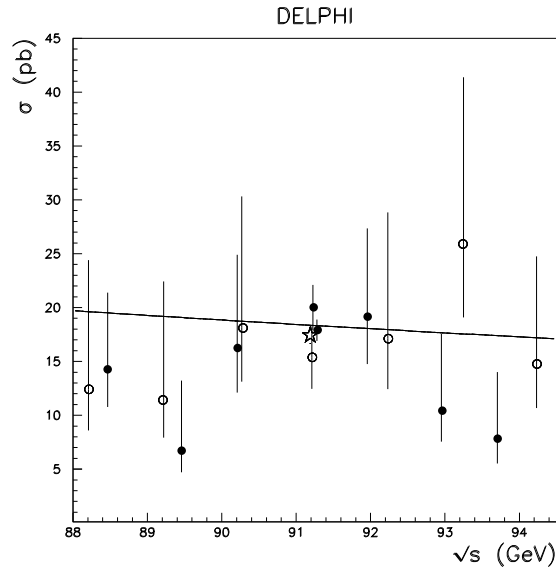


Figure 2: Total cross section (in pb) for the process $e^+e^- \rightarrow \gamma\gamma(\gamma)$ in the region $42^\circ < \theta < 90^\circ$, as a function of the LEP energy for the 1990 (open circles) and for 1991-92 data (black circles). The cross section at the mean of the centre-of-mass energies, weighted by the luminosity at each point, is also given (star). The solid line is the lowest order QED prediction.

prediction plus a Z^0 decay contribution, given by a Breit-Wigner line shape convoluted with an initial state radiator [16]. The peak cross section of the Z^0 term, which would be proportional to the partial width of the decay, was left as a free parameter. The effects of interference between the QED processes and these rare Z^0 decays were assumed to be negligible.

The distribution of the polar angle of the Z^0 decay products was assumed to have a $1 + \cos^2 \theta$ dependence and the global efficiencies for $Z^0 \rightarrow \gamma\gamma$, $Z^0 \rightarrow \pi^0\gamma$ and $Z^0 \rightarrow \eta\gamma$ were evaluated from Monte Carlo studies to be $(54.1 \pm 1.0)\%$, $(53.5 \pm 1.0)\%$ and $(37.4 \pm 0.8)\%$ respectively. These figures include the acceptance and the slightly different detection probabilities due to the different number of photons in the final states. The acceptance for the $\eta\gamma$ channel was obtained by considering only the neutral decay modes of the η .

A maximum likelihood fit to the total cross section, taking into account the same errors on the normalization as in the previous section, gave the following bounds at the 95% confidence level: $\text{BR}(Z^0 \rightarrow \gamma\gamma) < 5.5 \times 10^{-5}$, $\text{BR}(Z^0 \rightarrow \pi^0\gamma) < 5.5 \times 10^{-5}$ and $\text{BR}(Z^0 \rightarrow \eta\gamma) < 8.0 \times 10^{-5}$. The central values of the fitted widths were respectively: (-32 ± 75) keV, (-33 ± 76) keV and (-47 ± 110) keV.

From these measurements it is possible to derive limits on the Z^0 decay into a photon and other states having neutral decays to $\pi^0\gamma$ or $\eta\gamma$. The most significant limit is the one obtained for the $\omega\gamma$ channel: $\text{BR}(Z^0 \rightarrow \omega\gamma) < 6.5 \times 10^{-4}$ at the 95% confidence level.

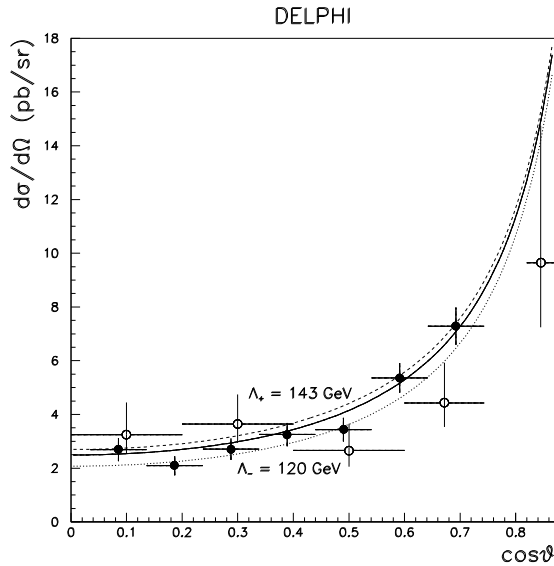


Figure 3: Differential cross section $d\sigma/d\Omega$ for the process $e^+e^- \rightarrow \gamma\gamma(\gamma)$ for 1990 (open circles) and for 1991-92 data (black circles). The solid line shows the lowest order QED prediction. The dashed (dotted) line shows the derived limit on the prediction parametrized by Λ_+ (Λ_-).

6 Search for compositeness.

The exchange of a virtual excited electron would modify the differential QED cross section [10]. A likelihood fit was performed to the following expression, as function of the mass of the excited electron (M_{e^*}) and the coupling constant (λ_γ):

$$\frac{d\sigma}{d\Omega} = \frac{\alpha^2}{s} \frac{1 + \cos^2 \theta}{1 - \cos^2 \theta} \left(1 + \frac{s^2 \lambda_\gamma^2}{2M_{e^*}^4} (1 - \cos^2 \theta) H(\cos^2 \theta) \right) \quad (2)$$

where $H(\cos^2 \theta) = a \frac{1 - \cos^2 \theta}{(1+a)^2 - \cos^2 \theta}$ and $a = 2M_{e^*}^2/s$. Fig. 4 shows the resulting 95% confidence level limit contour on the $(M_{e^*}, \lambda_\gamma/M_{e^*})$ plane. In the mass region below M_Z , a better limit was obtained from the DELPHI search for t-channel production of e^*e [17]. For $\lambda_\gamma = 1$, $M_{e^*} > 132 \text{ GeV}/c^2$ at the 95% confidence level, with a central value $1/M_{e^*}^4 = (-.24 \pm .22) \times 10^{-8} \text{ GeV}^{-4}$.

In some composite models the branching ratio $Z^0 \rightarrow \gamma\gamma\gamma$ can be as high as 2×10^{-4} , compared with the Standard Model prediction of 3×10^{-10} [18]. To study this particular decay mode, the selection criteria were modified in order to maximize the acceptance for this process and to keep the QED contribution as low as possible. In addition, in the case of a pure three body final state, the energies of the individual photons can be computed with good precision from the measurement of the particle directions after imposing energy-momentum conservation [17]. The energies of the photons were thus rescaled before applying the selection cuts. In detail, the selection criteria for three photon final state events were as follows :

- at least three electromagnetic clusters with $E > 10 \text{ GeV}$;
- at least two electromagnetic clusters in the region $42^\circ < \theta < 88^\circ$ or $92^\circ < \theta < 138^\circ$ and one in the region $20^\circ < \theta < 160^\circ$;

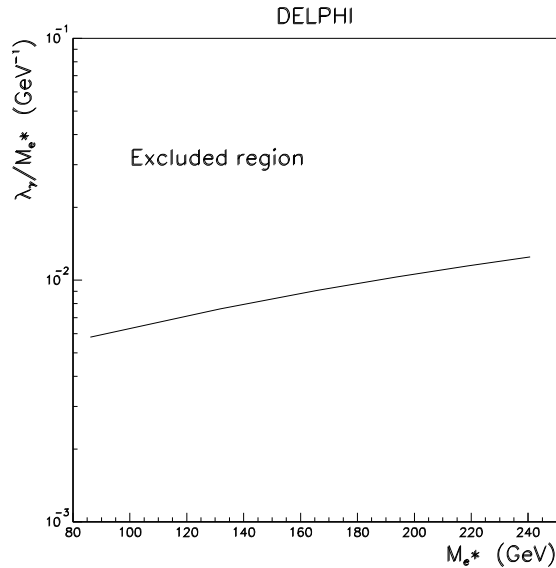


Figure 4: Upper limit on the effective coupling constant λ_γ/M_{e^*} versus M_{e^*} . For $M_{e^*} < M_Z$ a better limit is obtained by a direct search[17].

- the energy measured in the calorimeters (without rescaling) greater than 20 GeV for the most energetic cluster and greater than 2 GeV for the others;
- the cluster with the greatest measured energy had to be in the HPC;
- the opening angles between the third most energetic cluster and both the more energetic ones larger than 20° ;
- the sum of the opening angles between the three most energetic clusters larger than 359° , to avoid non planar events.

The requirements on the VD tracks and on the TK's were the same as in section 3. When there were two TK's in the same hemisphere, they were required to have an invariant mass smaller than $2 \text{ GeV}/c^2$. The cut on the measured energy at 2 GeV was introduced to ensure a good reconstruction of the shower position and, consequently, a precise energy rescaling. This was necessary because this selection accepts events with photons near the HPC boundaries. However, none of the selected events had actually a photon with such a low measured energy.

The number of selected events was 10 from the whole 1991-1992 sample. The number of expected events was assumed to be the sum of the QED contribution and a contribution proportional to the width of the $Z^0 \rightarrow \gamma\gamma\gamma$ decay. The former could be computed from the Monte Carlo program of Ref.[5] which was used to find both the cross section within the acceptance and, using 24046 fully simulated events, the selection efficiency. The total number of expected QED events was 7.3 ± 0.8 , where the error includes the statistical and systematic error on the efficiency, evaluated with the Monte Carlo program, and an additional normalization error of 10% to take into account the lack of radiative and higher order corrections in the predictions for this process.

The geometrical acceptance for $Z^0 \rightarrow \gamma\gamma\gamma$ was computed with a Monte Carlo program [19] and the selection efficiency was assumed to be equal to that of the QED channel. The global detection efficiency for a $Z^0 \rightarrow \gamma\gamma\gamma$ event was $(42.0 \pm 1.3)\%$. In the calculation of the number of expected events, the interference between the QED process and the

resonant decay was not taken into account. The normalization error for the expected events, considering the theoretical approximation and the efficiency evaluation, was 11%.

From these results a 95% confidence level upper limit for $\Gamma_{\gamma\gamma}$ of 41 keV was obtained, which corresponds to $BR(Z^0 \rightarrow \gamma\gamma\gamma) < 1.7 \times 10^{-5}$. The central value was $\Gamma_{\gamma\gamma} = 8.3_{-12.0}^{+15.2}$ keV and the likelihood curve is shown in Fig. 5.

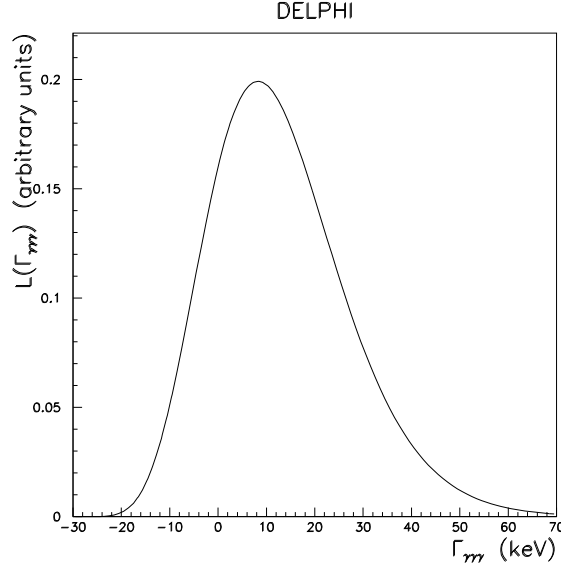


Figure 5: Likelihood curve for the fit to $\Gamma_{\gamma\gamma}$

7 Conclusions

The analysis of $e^+e^- \rightarrow \gamma\gamma(\gamma)$ cross sections shows good agreement with the QED predictions. Lower bounds were obtained on the QED cutoff parameters, $\Lambda_+ > 143$ GeV and $\Lambda_- > 120$ GeV, as well as on the mass of an excited electron: $M_{e^*} > 132$ GeV/ c^2 for $\lambda_\gamma = 1$. Upper limits have been set on the following processes :

$$BR(Z^0 \rightarrow \gamma\gamma) < 5.5 \times 10^{-5},$$

$$BR(Z^0 \rightarrow \pi^0\gamma) < 5.5 \times 10^{-5},$$

$$BR(Z^0 \rightarrow \eta\gamma) < 8.0 \times 10^{-5},$$

$$BR(Z^0 \rightarrow \omega\gamma) < 6.5 \times 10^{-4}$$

$$BR(Z^0 \rightarrow \gamma\gamma\gamma) < 1.7 \times 10^{-5}.$$

All the limits are at the 95% confidence level.

These results include the data published by DELPHI in a previous publication [1] which is superseded by this letter.

Acknowledgements

We are greatly indebted to our technical collaborators and to the funding agencies for their support in building and operating the DELPHI detector, and to the members of the CERN-SL Division for the excellent performance of the LEP collider. We thank F. Feruglio for useful discussions.

References

- [1] DELPHI collab., P. Abreu et al., Phys. Lett. **B268** (1991) 296.
- [2] OPAL collab., M.Z. Akrawy et al., Phys. Lett. **B257** (1991) 531;
ALEPH collab., D. Decamp et al., Physics Reports **216** (1992) 253;
L3 collab., B. Adeva et al., Phys. Lett. **B288** (1992) 404.
- [3] DELPHI collab., P. Aarnio et al., Nucl. Inst. and Meth. **A303** (1991) 233.
- [4] DELPHI collab., P. Abreu et al., Nucl. Phys. **B 367** (1991) 511.
- [5] F.A. Berends and R. Kleiss, Nucl. Phys. **B 186** (1981) 22.
- [6] DELPHI collab., "DELSIM, DELPHI Event Generation and Detector Simulation User's Guide", DELPHI note 89-67 (1989) unpublished.
- [7] F.A. Berends, W. Hollik and R. Kleiss, Nucl. Phys. **B 304** (1988) 712.
- [8] DELPHI collab., P. Abreu et al., "Measurement of the Lineshape of the Z^0 and Determination of Electroweak Parameters from its Hadronic and Leptonic Decays", CERN-PPE 94-08, to be published in Nucl. Phys. **B**.
- [9] B. Escoubes et al., Nucl. Inst. and Meth. **A257** (1987) 346.
- [10] D. Treille et al., preprint ECFA 87-108 in: ECFA Workshop on LEP 200, CERN report 87-08 Vol. 2, A. Böhm and W. Hoogland eds., (1987), 414.
- [11] S. Drell, Ann. Phys. (NY) **4** (1958) 75;
F.E. Low, Phys. Rev. Lett. **14** (1965) 238.
- [12] Particle Data Group, K. Hikasa et al., Phys. Rev. **D 45** part 2 (1992) III 39.
- [13] F. James and M. Roos, Phys. Rev. **D 44** (1991) 299.
- [14] C.N. Yang, Phys. Rev. **77** (1950) 242.
- [15] L. Arnellos et al., Nucl. Phys. **B 196** (1982) 378;
E.W.N. Glover et al., in: Z Physics at LEP 1, CERN report 89-08 Vol. 2, G. Altarelli and C. Verzegnassi eds., (1989) 1.
- [16] A. Borrelli et al., Nucl. Phys. **B 333** (1990) 357.
- [17] DELPHI collab., P. Abreu et al., Z. Phys. **C 53** (1992) 41.
- [18] F. Boudjema et al., in: Z Physics at LEP 1, CERN report 89-08 Vol. 2, G. Altarelli and C. Verzegnassi eds., (1989) 185.
- [19] M. Baillargeon and F. Boudjema, in "Workshop on Photon Radiation from Quarks", CERN report 92-04, S. Cartwright ed., (1992) 178.